Typical Meteorological Year Methodologies applied to solar spectral irradiance for PV applications

Jesús Polo [1]*, Miguel Alonso-Abella[1], Nuria Martín-Chivelet[1], Joaquín Alonso-Montesinos[2], Gabriel López[3], Aitor Marzo[4], Gustavo Nofuentes[5], Nieves Vela-Barrionuevo[1]

[1] Photovoltaic Solar Energy Unit (Energy Department e CIEMAT), Avda. Complutense 40, 28040 Madrid, Spain
[2] Department of Chemistry and Physics, University of Almería, 04120 Almería, Spain
[3] Dpto. Ingeniería Eléctrica y Térmica, de Diseño y Proyectos, Universidad de Huelva, Huelva, Spain
[4] Centro de Desarrollo Energético Antofagasta (CDEA), University of Antofagasta - Solar Energy Research Center, Antofagasta (Chile).
[5]IDEA Research Group, University of Jaén, Campus de Las Lagunillas, 23071 Jaén, Spain

* Corresponding author
Jesús Polo, email: jesus.polo@ciemat.es , Phone: +34 914962513, Fax : +34 913466037

Abstract

A Typical Meteorological Year (TMY) is frequently used in solar power for long-term energy yield analysis. Different approaches have been reported focusing on concentrating solar power or photovoltaic power plants that have established different relative contributions of the involved variables (mainly solar irradiance components and temperature) according to the application. For PV applications the estimation of the spectral gains and losses requires of on-site spectral measurements. Long-term analysis of the spectral influence on PV technologies has been performed for over seven years of measured spectral global tilted irradiance in Madrid. The experimental spectra were measured with an EKO spectroradiometer in the wavelength range of 300-1100 nm. The TMY methodology has been used to create a typical spectral year of global tilted irradiance that can be used for computing the spectral factor. This paper shows the different steps in applying the TMY methodology to spectral irradiance and the resulting spectral factors computed for seven different PV technologies. Thus, this approach can effectively be used to characterize the long-term spectral influence of PV technologies in a selected site.

Keywords: Spectral global tilted irradiance; Spectral factor; Typical Meteorological Year; PV modeling

1. Introduction

Solar power is a key element in the energy mix for the near future in order to mitigate the environmental consequences of fossil fuel consumption. Concentrating solar power (CSP) and Photovoltaic (PV) technologies are growing fast and an increase in the global penetration of both technologies (particularly PV) is foreseen in the short term. The design, dimensioning and financing stages of any solar power project needs prior knowledge and quantification of the expected energy at annual basis through a process commonly called yield-performance analysis. A yield-performance analysis basically consists of modeling the energy produced by the plant during a whole year as a case study to obtain a snapshot of the annual expected energy projected in the future and the associated uncertainty. This exercise requires a detailed knowledge of the meteorological inputs, mainly solar irradiance, for at least a whole year. Since inter-annual variability is expected in the meteorological conditions affecting the plant single Typical Meteorological Year (TMY) has been widely used as input to the plant model in PV and CSP technologies [1–8].

A TMY represents the long-term characteristics of a set of meteorological variables in the form of a time series (hourly or sub-hourly) for a whole year. The idea of creating an artificial year was conceived at Sandia National Laboratory and they proposed a procedure for concatenating measured data from 12 months (January to December) selected as typical for constructing the artificial year [9]. Despite different methodologies for selecting the typical months proposed elsewhere, the Sandia approach is probably the most extensively used [10–16]. In all the methodologies for TMY the contribution of the involved meteorological variables is relatively weighted. However, different choices for the weights of the selected meteorological variables can be used and have also been proposed by several authors using the basis of the Sandia procedure [3,7,12,17–22]. Moreover, specific TMY focused on the technology through the selection of variables and weights have been also proposed and discussed recently. Thus Typical Global Year (TGY) and Typical Direct year (TDY) were recently proposed by NREL and compared with the general TMY [8]. Similarly, a Typical Yield Year was proposed based on the statistical analysis of multi-year modeling energy output data for CSP and PV [3,18,23].

The spectral characteristics of the incoming solar irradiance strongly depend on local factors, such as atmospheric aerosol, water vapor content, air mass and others. The study of the incoming spectral irradiance is of high interest in all solar technologies [24–26]. The shape of the solar spectrum affects the outdoor performance of PV modules due to the selective spectral response of PV technologies. The efficiency of PV modules is determined at laboratory level under a specific insolation and temperature conditions denoted as standard test conditions (STC). STC is represented by an incident solar irradiance of 1000 W m^{-2}, module temperature of 25 °C and a reference spectral distribution of irradiance. The reference spectral irradiance commonly used is the ASTM G173 for an air mass of 1.5 and very specific conditions of the atmospheric attenuants [27–29]. However, the on-site incoming spectral irradiance that impinges on PV devices usually differs from the reference spectrum and presents seasonal and daily variations. Consequently, energy conversion occurs at spectral distributions that differ from the reference resulting in different efficiency values from those corresponding to STC. This difference, or spectral-related mismatch, is known as the spectral mismatch error and has an influence on the short-circuit current, maximum power, fill factor and efficiency, which can vary depending on the PV technology [30,31]. Spectral mismatches can be characterized by computing the spectral factor (SF) with experimental spectral irradiance data [30,32,41–43,33–40]. In absence of experimental spectral data an alternative approach is to estimate the incoming spectral irradiance with radiative transfer models [44,45]. However, this alternative approach is limited to clear-sky conditions. Maps of geographical variation in the annual average spectral mismatch were presented recently by several authors using satellite-based solar radiation-modeled data [44,46]. The Simple Model of Atmospheric Radiative Transfer of Sunshine (SMARTS) [47–49] was used at five locations of the Aerosol Robotic Network (AERONET) [50] to assess the influence of the spectrum on the energy output of high concentrator PV and conventional PV technology [34].

Despite TMY methodologies have extensively been used in different ways, delivering time series of broadband solar radiation data for the performance modeling of solar systems, there is no prior work on using TMY approaches for characterizing the spectral effects in PV performance. Therefore, this paper presents an analysis of the methodology for building TMYs applied to generate an artificial year of spectral global tilted irradiance for Madrid, as a novel contribution to the solar energy community. The statistical approach to select the monthly candidates from the sample (over 6 years of spectral measurements) from the Sandia methodology was used. The typical spectral year was used to compute the spectral factor for seven PV technologies and compared to the long term spectral factors computed from the individual spectra with high agreement evidencing that the TMY methodology can be extended to the spectral global tilt irradiance.

2. Data description and preprocessing

Spectral global tilt irradiance measurements, south oriented and 30° of inclination angle have been collected from 6th May 2012 to 13th March 2019 at a rooftop of a university building in Madrid (40.45 N, -3.72 E). Spectral data, in watts per square meter per nanometer, were measured with a spectroradiometer (EKO MS-711) working in the spectral range of 300-1100 nm, with an optical resolution (FWHM) < 7 nm. The acquisition system was programmed to continuously store spectral data every 5 minutes. Therefore, a database of around 220,000 spectra was available for this work. For all the individual spectra, the average energy per photon (*APE*) index was calculated in order to have a single parameter that might help in filtering spectral data and gather the spectral characteristics into one single parameter as well.

Jardine et al. [51], first proposed the *APE* as the ratio of the total irradiance of the spectrum to the photon flux density and it is written as:

$$APE\ (eV) = \frac{\int_{\lambda 1}^{\lambda 2} G(\lambda) d\lambda}{q \int_{\lambda 1}^{\lambda 2} \phi(\lambda) d\lambda} \tag{1}$$

where λ_1 (nm) and λ_2 (nm) are the lower and upper wavelength limits, respectively, of the considered waveband, q is the electronic charge (1.602x10^{-19} eVC), G is the spectral irradiance and ϕ the photon spectral flux density defined as:

$$\phi(\lambda) = \frac{G(\lambda)\lambda}{h\ c} \tag{2}$$

where *h* is the Planck's constant and *c* the speed of light in vacuum. The value of *APE* for the AM1.5G reference spectrum equals 1.83 eV for the 300–1100 nm waveband. Therefore, values of this index higher or smaller than that calculated under reference conditions indicate a 'blue' or 'red shift' in the spectral distribution under scrutiny, respectively. *APE* was conceived as a unique parameter representing the spectral tilt irradiance [36] and even though it is clear that it represents somewhat the spectral characteristics of solar irradiance there are still doubts in the scientific community about the uniqueness of the relationship [38,52].

In addition, hourly clear-sky global tilt spectral irradiance was computed for a whole year at hourly basis with SMARTS2 for the site. SMARTS2 has become a reference radiative transfer model for computing spectral irradiance components at ground level [47,49]. Precipitable water and aerosol optical depth (AOD) minimum values were taken from CAMS (https://atmosphere.copernicus.eu/) retrievals in order to have an estimation of the maximum clear-sky tilt spectra along a complete year in Madrid. *APE* index was also computed for these hourly clear-sky spectra obtained with the SMARTS2 model.

Thus, the *APE* index is used in this work as quality control method to detect wrong experimental spectra. The filtering criterion used here was to reject all measured spectra whose *APE* was 1.5 times higher than the maximum *APE* for clear-sky conditions computed from SMARTS, since it was observed that this threshold was enough to reject erroneous spectra without altering the apparently good ones. Nevertheless, spectra were properly measured and filtering process removed only 9 spectra with APE values far beyond the expected variability range (about 1.2 to 2.3 for the spectral range of 300-1100, and mid-latitudes, according to experimental information found in literature) [53,54]. Thus 9 measured spectra with *APE* values greater than 2.7 were rejected. Figure 1 shows the result of this filtering process; on the left individual experimental spectra are plotted showing several errors in the measuring process and on the right plot the filtered spectra show the removal of the erroneous data; the figure shows also an example of erroneous spectrum with an *APE* value of 14.5 and showing also irradiances in the UV range much higher than the expected clear-sky values. Figure 2 plots the individual *APE* index of the filtered spectra. The *APE* index of the standard spectrum ASTM G173 is 1.83 eV and that for the experimental spectral data varies in the range 1.6-2.2 eV showing the differences with respect to the ASTM G173. Figure 2, thus, illustrates the range of variability of APE in the database; all APE values are within the physically expected range.

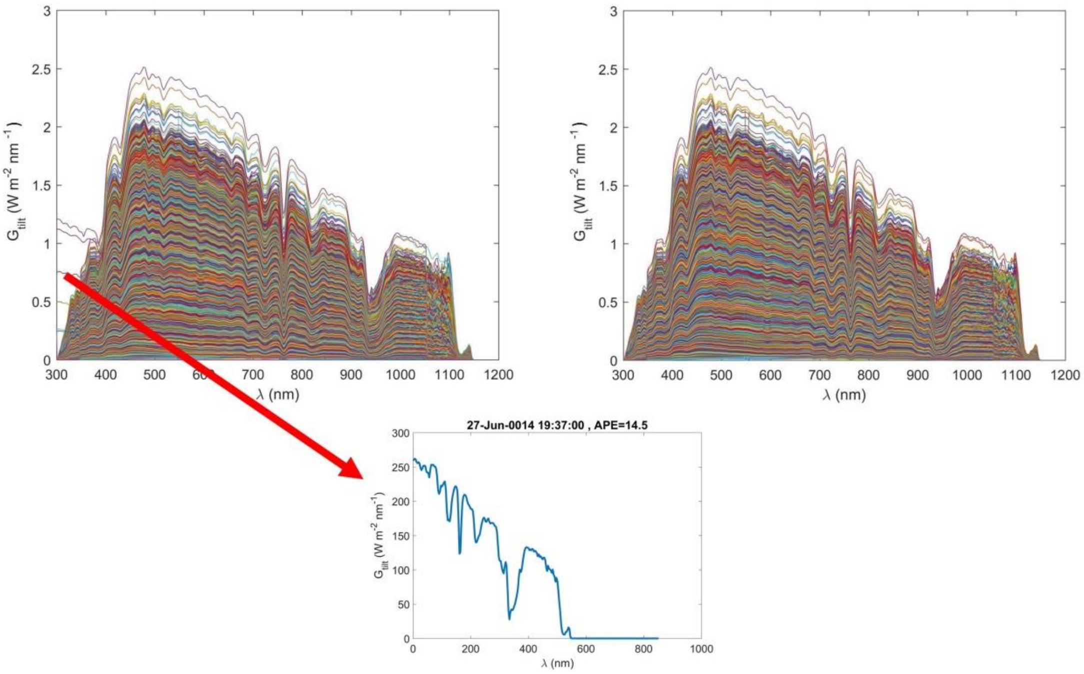

Fig. 1. Individual measured spectra (left). Filtered measured spectra (right). Example of a single wrong spectrum that was filtered (bottom).

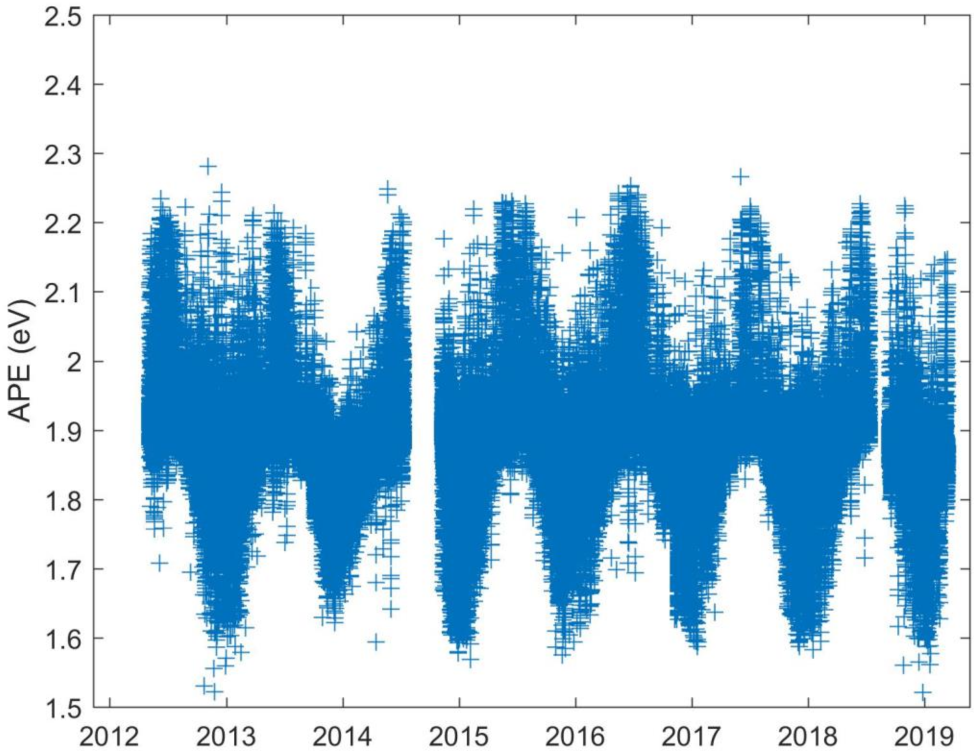

Fig. 2. The *APE* index computed for the individual filtered spectra of the measured database

3. Methdology

3.1 Spectral Factor determination

The spectral factor (SF) is a measure of the relative performance of a PV module that is being exposed to a spectral irradiance different to the reference spectrum (e.g. STC conditions). Therefore, SF can be considered as an estimator of the relative energy gains or losses associated with the spectral characteristics of the incoming solar radiation. According to the International Electrochemical Commission (IEC) SF is defined as [55],

$$SF = \frac{\int G(\lambda)SR(\lambda)d\lambda \ \int G_{ref}(\lambda)d\lambda}{\int G_{ref}(\lambda)SR(\lambda)d\lambda \ \int G(\lambda)d\lambda} \tag{3}$$

where G_{ref} and G refer to the spectral irradiance of the standard reference (ASTM G173) and measured spectra, respectively, and SR is the spectral response of the PV module. The spectral response is the ratio of the current generated by the solar cell to the power incident on the solar cell, as a function of the wavelength. According to this expression spectral gains imply values of SF higher than 1, while spectral losses lead to values of SF lower than 1.

Seven different PV technologies have been considered in this work, which were already used in other studies and were previously characterized in the CIEMAT PV laboratory [32]. The spectral response of each technology used here is shown in Figure 3; these technologies are: a-Si (amorphous silicon), CIS (copper indium diselenide), HIT (heterojunction with intrinsic thin layer), p-Si (polycrystalline or multicrystalline silicon), EFG (edge fed growth silicon), CdTe (cadmium telluride) and m-Si BCC (back-contact mono- crystalline silicon). The values of the SF for each of the seven technologies have been computed with Expression 3 for all individual filtered spectra of the measured database.

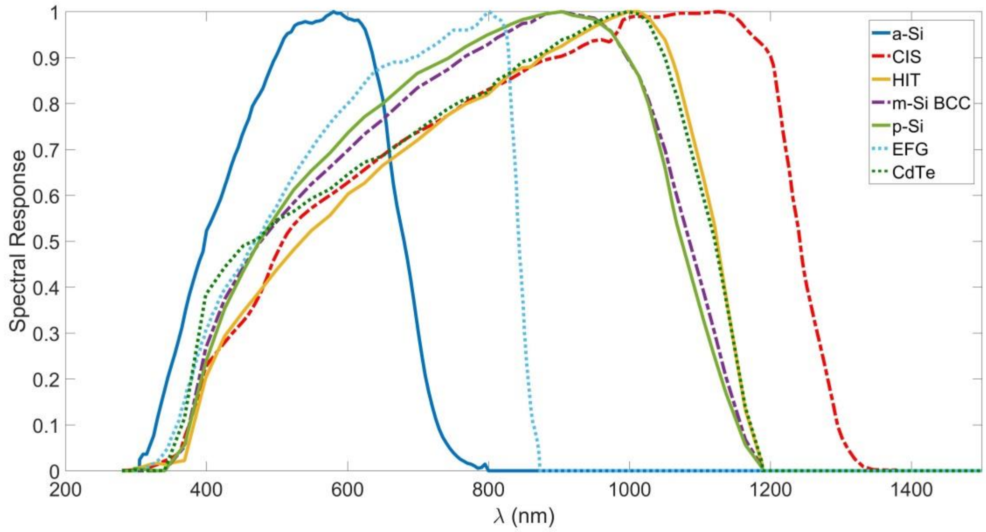

Fig. 3. Spectral response of seven different technologies measured at CIEMAT

3.2 Typical Meteorology Year methodology

One of the most successful and widely used methodologies for constructing a TMY is the Sandia Lab method, which is based upon the Finkelstein-Schafer (FS) statistic for selecting the individual month candidates [56]. The FS statistic for a meteorological variable *X* to be considered in the TMY is defined as:

$$FS_X(y,m) = \frac{1}{N}\sum_{i=1}^{N}\left|CDF_m(X_i) - CDF_{y,m}(X_i)\right| \tag{4}$$

where CDF_m is the long-term cumulative distribution function of the daily values of the variable X for month m, $CDF_{y,m}$ is the short-term (corresponding to year y) cumulative distribution function of the daily values of *X*, and *N* is the number of bins. The month candidate is the corresponding to the minimum value of the weighted sum (WS) of the FS statistics corresponding to each meteorological variable considered.

$$WS(y,m) = \sum_{j=1}^{M} W_j \; FS_j(y,m) \tag{5}$$

where W_j is the relative weight of the variable *j* and *M* is the number of variables involved. Seven different TMYs have been constructed in this work by selecting different combinations of weights and variables according to the purpose of the TMY and the literature review.

In this work two variables have been considered, with the same relative weight, to determine the typical global tilt spectral irradiance: the integral of the spectral irradiance limited to the experimental wavelength range (300-1100 nm), denoted here as GTI, and the APE index. The first variable was intended to account for the inter-annual variability associated with cloud transmission. The APE index would represent, thus, the inter-annual variability due to other main atmospheric components or attenuants that affect the spectral distribution (aerosols and precipitable water mainly). Therefore, the typical spectral year results from the concatenation of the months that fulfill the condition of minimum WS:

$$WS(y,m) = 0.5\, FS_{GTI}(y,m) + 0.5\, FS_{APE}(y,m) \tag{6}$$

4. Results and Discussion

The initial database for this study consisted of over 200,000 5-minute values of four main variables: GTI, APE index and SF for 7 different technologies and global tilt spectral irradiance, covering the period from 2012 to 2019. In the whole measuring period there were gaps in the data due to system shutdown, failures in the acquisition and so on, as well as some other conditions associated with the rejected data considered as wrong measurements. The data of these four main variables, considered as valid data, were aggregated to hourly means.

Since the statistical analysis for computing the FS statistic is performed on daily basis, daily means of the main variables used in this study were estimated from the hourly mean values. The cumulative distribution functions (CDFs) of the two involved variables (GTI and APE) were estimated by using the kernel density estimation (KDE) with the daily values. The KDE is a non-parametric way to estimate the probability density function of a random variable that is widely used and offers some advantages in computing the distribution function [57]. Figure 4 shows the CDF daily values of GTI and *APE* for each month of the year.

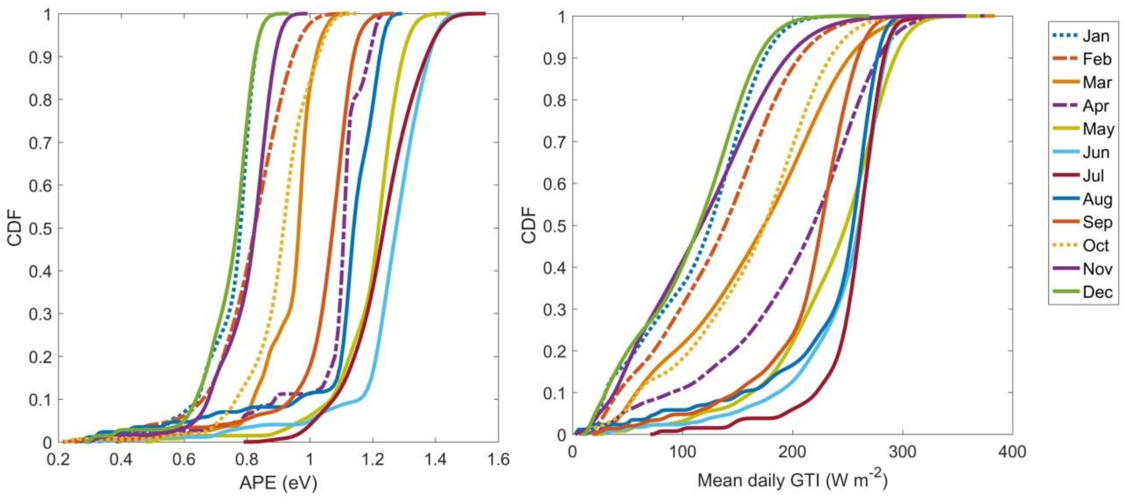

Fig. 4. CDF of daily GTI and *APE* for each month of the year

The Sandia Lab methodology was applied to the daily means data of the selected variables to determine the month candidate to be part of the typical meteorological or reference year. Table 1 shows the resulting month candidates.

Table 1. List of the candidate months to be part of the TMY for spectral irradiance

Month	Jan	Feb	Mar	Apr	May	Jun	Jul	Aug	Sep	Oct	Nov	Dec
Year	2013	2013	2014	2014	2014	2017	2012	2012	2012	2012	2014	2016

The TMY for spectral tilted irradiance is then formed by concatenating the hourly spectral irradiance measured data according to the monthly distribution listed in Table 1. In other words the TMY data for January are the spectral data of January 2013, for February are the spectral data of February 2013, for March are the spectral data of March 2014 and so on. As a result we have 8760 spectra covering each hour of the TMY. Figure 5 shows the hourly mean values of the spectral TMY of global tilted irradiance. Likewise, since the work is particularly focused on PV applications, the same procedure was followed to create 8760 values of the SF for each of the seven technologies included in this work, which constitutes a representative year of hourly SFs for each technology, which we have denominated a TMY of spectral factors. Figure 6 illustrates, using intensity plots, the TMY of the SF for each technology.

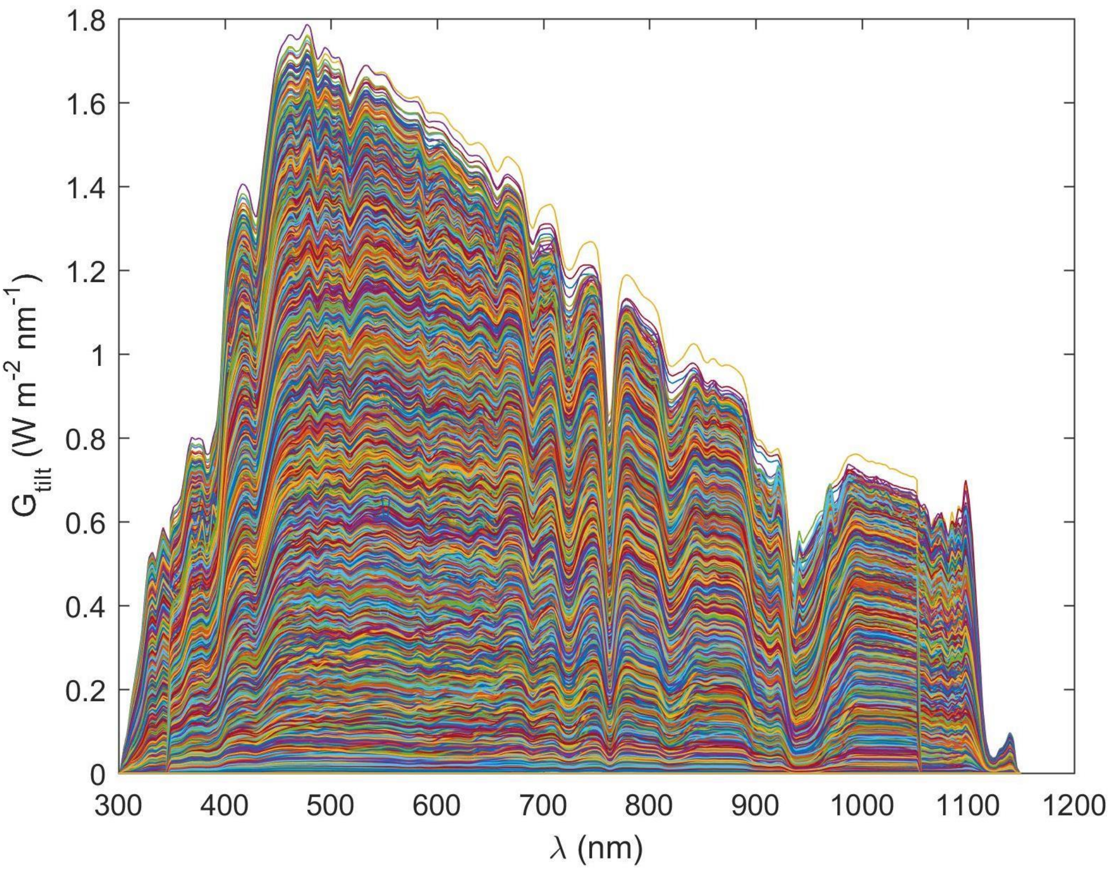

Fig.5. TMY for spectral global tilt irradiance (8760 spectra)

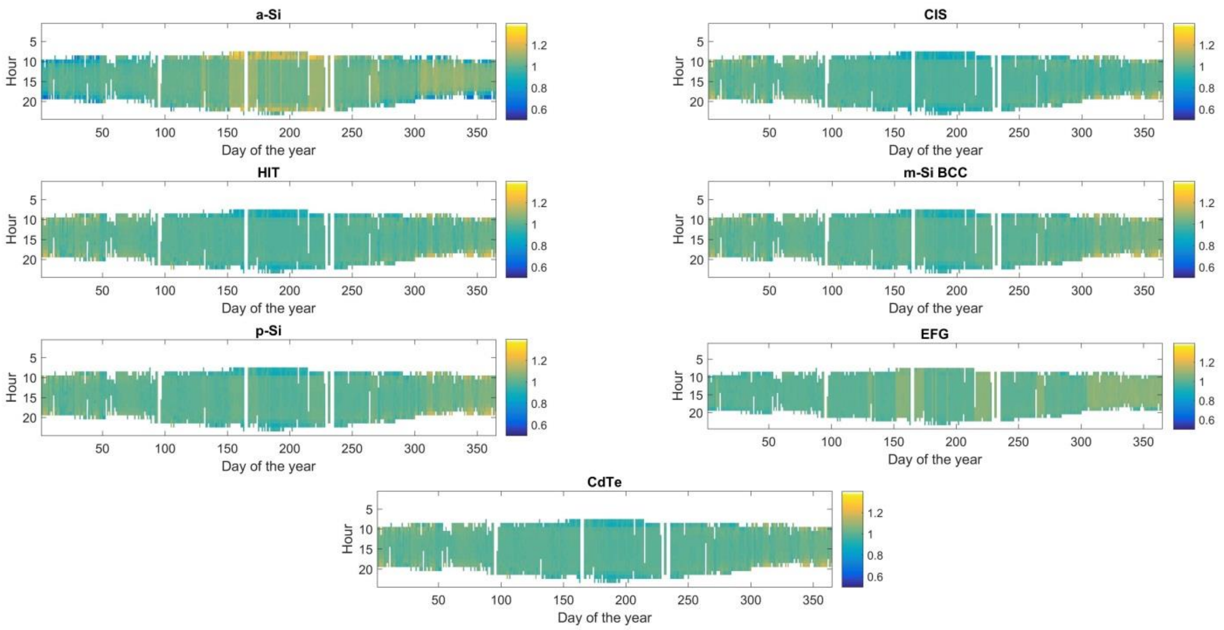

Fig.6. Intensity plots of the typical SF for seven PV technologies

Therefore, the Sandia methodology to build TMY can be used effectively for creating the long-term year of SF for PV technologies by concatenating the individual hourly SFs of the candidate months. In order to explore the robustness and coherence of the methodology for computing the long-term year of SF a different approach could also be used. Since a TMY of spectral global tilt irradiance has been built from experimental data, the associated SFs can also be computed from the spectral TMY using Equation 3, where G spectral data used are the spectral TMY of global tilt. Figure 7 shows the scatter plots of the SFs computed with the spectral irradiance TMY (in the x-axis) compared to the SFs resulted from the concatenation of individual hourly SFs for the whole period of measurements (in the y-axis). These scatter plots show that both methodologies are practically equivalent. The mean bias deviation between both procedures was in all the PV technologies below 0.4 % and the root mean square deviations were below 1.5 % in all the cases except for the a-Si SF which was 4%. In order to quantify the differences of the long-term SF computed from spectral TMY and from statistical long-term of all the individual SFs, in addition to the scatter plots of Figure 7, in the Table 2 several statistical performance parameters are listed for each technology used in this work showing a rather good performance in most technologies (the largest differences were found in the a-Si technology). The statistical metrics selected were computed according to a recent review of statistical performance indicators by Gueymard [58]. The computed metrics are: Mean Bias difference (*MBD*), Root Mean Squared Difference (*RMSD*), Mean Absolute Difference (*MAD*) and Coefficient of Determination (R^2).

In order to quantify the spectral gains or losses of the spectral TMY the cumulative annual estimation of the SF is calculated for each of the seven PV technologies analyzed here. The SF for a period of time, a year in this case, is estimated using the following expression [32,44]:

$$SF_{year} = \frac{G^* \sum_{h=1}^{8760} \int G_h(\lambda) SR(\lambda) d\lambda}{I_{SC}^* \sum_{h=1}^{8760} \int G_h(\lambda) d\lambda} \tag{7}$$

Table 2. Statistical Metrics for the SF in percentage

Technology	*MBD*	*RMSD*	*MAD*	*R^2*
a-Si	-0.12	4.04	0.83	0.78
CIS	0.327	1.38	0.52	0.88
HIT	0.35	1.43	0.54	0.88
m-Si BCC	0.31	1.12	0.43	0.90
p-Si	0.31	1.12	0.43	0.91
EFG	0.14	0.79	0.23	0.94
CdTe	0.27	1.04	0.38	0.89

where G^* is the integral of the standard global tilt spectrum from the ASTM G 173 within the wavelength range of this study (300-1100 nm) and I_{SC}^* is:

$$I_{SC}^* = \int_{300}^{1100} G_{ref}(\lambda) SR(\lambda) d\lambda \tag{8}$$

Table 3 shows the annual values of the SF for each PV technology showing a very balanced SF long-term annual value, as it was also illustrated in Figure 6. These results showing an annual spectral factor below 2% in mid-latitude European sites like Madrid are in good agreement to other recent studies [39,46].

Table 3. Annual SF associated with the spectral TMY

Technology	a-Si	CIS	HIT	m-Si BCC	p-Si	EFG	CdTe
SF	1.02	0.99	1.00	1.01	1.01	1.02	1.00

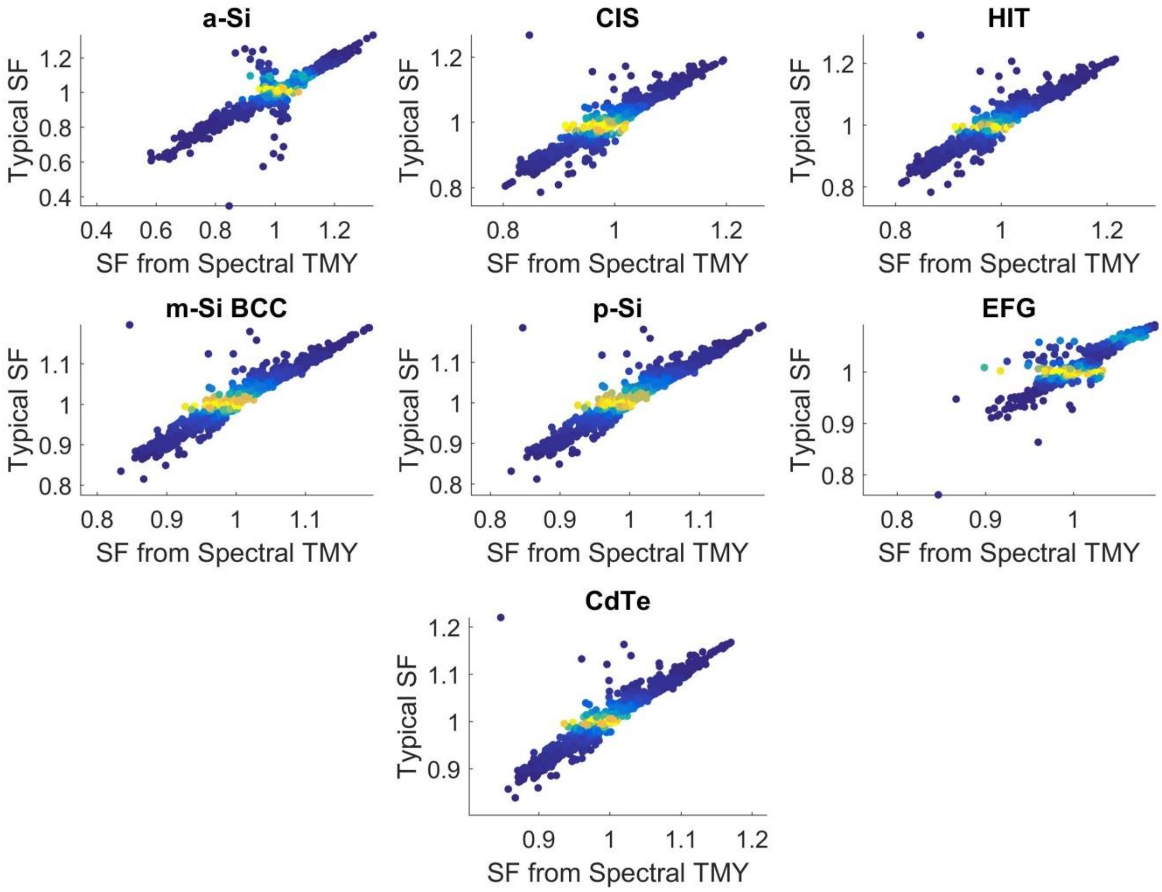

Fig.7. Scatter plots for the SF computed from TMY and from individual data.

5. Conclusions

The long-term characterization of the global tilted spectral irradiance results of interest for determining the expected spectral gains or losses of PV technologies in the performance for the plant operational life. Typical meteorological year methodologies, such as the Sandia one, have been used extensively to create TMYs for the main meteorological variables involved in solar energy systems performance. In several cases the methodology has been used on the broadband solar irradiance components and temperature only, also focusing on the use of TMY in solar power plant long term performance. Aimed at PV applications and at determining the long-term spectral effects on the PV technologies in this work the TMY methodology was used to generate a typical year of spectral global tilted irradiance. Two simple variables that can be computed directly from the spectrum have been used: the integral that represents the broadband global tilted irradiance in the spectral range and is associated to cloud induced variability, and the average photon energy which would represent the variability associated with other atmospheric attenuants like aerosols, ozone and water vapor.

An artificial year of 8760 hourly spectra of global tilted irradiance, denoted as spectral TMY, has been created by concatenating statistical representative months of experimental spectra in Madrid according to the Sandia methodology. This year would represent the long term spectral characteristics of solar irradiance at the site. The spectral factor for seven different PV technologies was computed with both the TMY and all the individual measured spectra for the sampling period. The statistical comparison showed that the methodology for creating TMY can be applied to global tilted spectral irradiance for PV applications resulting in coherent estimations of the spectral gains and losses.

Acknowledgements

The authors would like to thank the PVCastSOIL Project (ENE2017-83790-C3-1, 2 and 3), which is funded by the Spanish Ministry of Economy and Competitiveness and co-financed by the European Regional Development Fund. The authors also acknowledge CONICYT/FONDAP/15110019 “Solar Energy Research Center” SERC-Chile project, and the Chilean Economic Development Agency (CORFO) with contract No 17PTECES-75830 under the framework of the project “AtaMoS TeC”. Finally, the corresponding author wish to acknowledge the fruitful discussions and collaborative work done within the task 16 IEA-PVPS where solar spectral modeling and measuring is one topic of interest.

References

[1] Lara-Fanego V, Pulgar-Rubio J, Fernández-Peruchena C, Gastón-Romeo M, Moreno-Tejera S, Ramírez-Santigosa L, et al. A novel procedure for generating solar irradiance TSYs. AIP Conference Proceedings 2017;1850. doi:10.1063/1.4984523.

[2] Hirsch T, Dernsch J, Fluri T, García-Barberena J, Giuliano S, Hustig-Diethelm F, et al. SolarPACES Guideline for Bankable STE Yield Assessment. IEA Technology Collaboration Programme SolarPACES: 2017.

[3] Kulesza K. Comparison of typical meteorological year and multi-year time series of solar conditions for Belsk, central Poland. Renewable Energy 2017;113:1135–40. doi:10.1016/j.renene.2017.06.087.

[4] Murphy S. The construction of a modified Typical Meteorological Year for photovoltaic modeling in India. Renewable Energy 2017;111:447–54.

[5] Pagh Nielsen K, Blanc P, Vignola F, Ramírez L, Blanco M, Meyer R. Discussion of current used practices for: Creation of Meteorological Data Sets for CSP/STE Performance Simulations. Technical Report SolarPACES Task V: 2017.

[6] Pelland S, Maalouf C, Kenny R, Leahy L, Schneider B, Bender G. Solar Energy Assessments: When Is a Typical Meteorological Year Good Enough? Proceedings of the Solar 2016 Conference 2016:1–7. doi:10.18086/solar.2016.01.17.

[7] Cebecauer T, Suri M. Typical Meteorological Year Data: SolarGIS Approach. Energy Procedia 2015;69:1958–69. doi:10.1016/j.egypro.2015.03.195.

[8] Habte A, Lopez A, Sengupta M, Wilcox S. Temporal and Spatial Comparison of Gridded TMY, TDY, and TGY Data Sets. NREL/TP-5D00-60886, National Renewable Energy Lab Report, Golden Co,: 2014.

[9] Hall IJ, Prairie RR, Anderson HE, Boes EC. Generation of typical meteorological years for 26 SOLMET stations. Albuquerque (USA): 1978.

[10] Marion W, Urban K. User’s Manual for TMY2s. Typical Meteorological Years. vol. NREL/TP-46. Golden CO: NREL/TP-463-7668, National Renewable Enery Laboratory; 1985.

[11] Argiriou A, Lykoudis S, Kontoyiannidis S, Balaras CA, Asimakopoulos D, Petrakis M, et al. Comparison of methodologies for tmy generation using 20 years data for Athens, Greece. Solar Energy 1999;66:33–45.

[12] Lhendup T, Lhundup S. Comparison of methodologies for generating a typical meteorological year (TMY). Energy for Sustainable Development 2007;11:5–10. doi:10.1016/S0973-0826(08)60571-2.

[13] Ohunakin OS, Adaramola MS, Oyewola OM, Fagbenle RO. Generation of a typical meteorological year for north–east, Nigeria. Applied Energy 2013;112:152–9. doi:10.1016/j.apenergy.2013.05.072.

[14] Yang L, Lam JC, Liu J. Analysis of typical meteorological years in different climates of China. Energy Conversion and Management 2007;48:654–68. doi:10.1016/j.enconman.2006.05.016.

[15] Bre F, Fachinotti VD. Generation of typical meteorological years for the Argentine Littoral Region. Energy and Buildings 2016;129:432–44. doi:10.1016/j.enbuild.2016.08.006.

[16] Lam JC, Hui SCM, Chan ALS. A Statistical Approach to the Development of a Typical Meteorological Year for Hong Kong. Architectural Science Review 1996;39:201–9. doi:10.1080/00038628.1996.9696818.

[17] Realpe AM, Vernay C, Pitaval S, Lenoir C, Blanc P. Benchmarking of five typical meteorological year datasets dedicated to concentrated-PV systems. Energy Procedia 2016;97:108–15. doi:10.1016/j.egypro.2016.10.031.

[18] Polo J, Fernández-Peruchena C, Gastón M. Analysis on the long-term relationship between DNI and CSP yield production for different technologies. Solar Energy 2017;115:1121–9. doi:10.1016/j.solener.2017.07.059.

[19] Skeiker K. Generation of a typical meteorological year for Damascus zone using the Filkenstein–Schafer statistical method. Energy Conversion and Manegement 2004;45:99–112. doi:10.1016/S0196-8904(03)00106-7.

[20] Janjai S, Deeyai P. Comparison of methods for generating typical meteorological year using meteorological data from a tropical environment. Applied Energy 2009;86:528–37. doi:10.1016/j.apenergy.2008.08.008.

[21] Markou MT, Kambezidis HD, Bartzokas A, Darula S, Kittler R. Generation of daylight reference years for two European cities with different climate: Athens, Greece and Bratislava, Slovakia. Atmospheric Research 2007;86:315–29. doi:10.1016/J.ATMOSRES.2007.07.001.

[22] Petrakis M, Kambezidis HD, Lykoudis S, Adamopoulos AD, Kassomenos P, Michaelides IM, et al. Generation of a “typical meteorological year” for Nicosia, Cyprus. Renewable Energy 1998;13:381–8. doi:10.1016/S0960-1481(98)00014-7.

[23] Espinar B, Blanc P, Wald L. Report on the producction S4 “TMY FOR PRODUCTION.” Project ENDORSE 2012:12.

[24] Marzo A, Ferrada P, Beiza F, Besson P, Alonso-Montesinos J, Ballestrín J, et al. Standard or local solar spectrum? Implications for solar technologies studies in the Atacama desert. Renewable Energy 2018;127:871–82. doi:10.1016/J.RENENE.2018.05.039.

[25] Jessen W, Wilbert S, Gueymard CA, Polo J, Bian Z, Driesse A, et al. Proposal and evaluation of subordinate standard solar irradiance spectra for applications in solar energy systems. Solar Energy 2018;168:30–43. doi:10.1016/J.SOLENER.2018.03.043.

[26] Marzo A, Polo J, Wilbert S, Gueymard CA, Jessen W, Ferrada P, et al. Sunbelt spectra comparison with standard ASTM G173: The Chilean case. AIP Conference Proceedings, vol. 2033, AIP Publishing LLC ; 2018, p. 190010. doi:10.1063/1.5067195.

[27] IEC 60904-3. Photovoltaic devices - Part 3: Measurement principles for terrestrial photovoltaic (PV) solar devices with reference spectral irradiance data. 2016.

[28] Gueymard CA, Myers D, Emery K. Proposed reference irradiance spectra for solar energy systems testing. Solar Energy 2002;73:443–67. doi:10.1016/S0038-092X(03)00005-7.

[29] ASTM G173(03). Standard Tables for Reference Solar Spectral Irradiances: Direct Normal and Hemispherical on 37° Tilted Surface. 2012. doi:10.1520/G0173-03R12.

[30] Nofuentes G, García-Domingo B, Muñoz J V., Chenlo F. Analysis of the dependence of the spectral factor of some PV technologies on the solar spectrum distribution. Applied Energy 2014;113:302–9. doi:10.1016/j.apenergy.2013.07.044.

[31] Cornaro C, Andreotti A. Influence of Average Photon Energy index on solar irradiance characteristics and outdoor performance of photovoltaic modules. Progress in Photovoltaics: Research and Applications 2012;21:n/a-n/a. doi:10.1002/pip.2194.

[32] Alonso-Abella M, Chenlo F, Nofuentes G, Torres-Ramírez M. Analysis of spectral effects on the energy yield of different PV (photovoltaic) technologies: The case of four specific sites. Energy 2014;67:435–43. doi:10.1016/j.energy.2014.01.024.

[33] Eltbaakh YA, Ruslan MH, Alghoul MA, Othman MY, Sopian K. Measurements of spectral-band solar irradiance in Bangi, Malaysia. Solar Energy 2013;89:62–80. doi:http://dx.doi.org/10.1016/j.solener.2012.11.016.

[34] Fernández EF, Almonacid F, Ruiz-Arias JA, Soria-Moya A. Analysis of the spectral variations on the performance of high concentrator photovoltaic modules operating under different real climate conditions. Solar Energy Materials and Solar Cells 2014;127:179–87. doi:10.1016/j.solmat.2014.04.026.

[35] Ishii T, Otani K, Takashima T, Xue Y. Solar spectral influence on the performance of photovoltaic (PV) modules under fine weather and cloudy weather conditions. Progress in Photovoltaics: Research and Applications 2011:n/a-n/a. doi:10.1002/pip.1210.

[36] Minemoto T, Nakada Y, Takahashi H, Takakura H. Uniqueness verification of solar spectrum index of average photon energy for evaluating outdoor performance of photovoltaic modules. Solar Energy 2009;83:1294–9. doi:10.1016/j.solener.2009.03.004.

[37] Minemoto T, Nagae S, Takakura H. Impact of spectral irradiance distribution and temperature on the outdoor performance of amorphous Si photovoltaic modules. Solar Energy Materials and Solar Cells 2007;91:919–23. doi:10.1016/j.solmat.2007.02.012.

[38] Nofuentes G, Gueymard C, Aguilera J, Charte F. Is the average photon energy a unique characteristic of the spectral distribution of global irradiance? Solar Energy 2017;149:32–43. doi:10.1016/j.solener.2017.03.086.

[39] Nofuentes G, de la Casa J, Solís-Alemán EM, Fernández EF. Spectral impact on PV performance in mid-latitude sunny inland sites: Experimental vs. modelled results. Energy 2017;141:1857–68. doi:10.1016/J.ENERGY.2017.11.078.

[40] Okullo W, Munji MK, Vorster FJ, van Dyk EE. Effects of spectral variation on the device performance of copper indium diselenide and multi-crystalline silicon photovoltaic modules. Solar Energy Materials and Solar Cells 2011;95:759–64. doi:10.1016/j.solmat.2010.10.018.

[41] Pérez-López JJ, Fabero F, Chenlo F. Experimental solar spectral irradiance until 2500 nm: results and influence on the PV conversion of different materials. Progress in Photovoltaics: Research and Applications 2007;15:303–15. doi:10.1002/pip.739.

[42] Senthilarasu S, Fernández EF, Almonacid F, Mallick TK. Effects of spectral coupling on perovskite solar cells under diverse climatic conditions. Solar Energy Materials and Solar Cells 2015;133:92–8. doi:10.1016/j.solmat.2014.10.037.

[43] Sirisamphanwong C, Ketjoy N. Impact of spectral irradiance distribution on the outdoor performance of photovoltaic system under Thai climatic conditions. Renewable Energy 2012;38:69–74. doi:10.1016/j.renene.2011.07.008.

[44] Polo J, Alonso-Abella M, Ruiz-Arias JA, Balenzategui JL. Worldwide analysis of spectral factors for seven photovoltaic technologies. Solar Energy 2017;142:194–203. doi:10.1016/j.solener.2016.12.024.

[45] Núñez R, Jin C, Victoria M, Domínguez C, Askins S, Herrero R, et al. Spectral study and classification of worldwide locations considering several multijunction solar cell technologies. Progress in Photovoltaics: Research and Applications 2016;24:1214–28. doi:10.1002/pip.2781.

[46] Amillo A, Huld T, Vourlioti P, Müller R, Norton M, Amillo AMG, et al. Application of Satellite-Based Spectrally-Resolved Solar Radiation Data to PV Performance Studies. Energies 2015;8:3455–88. doi:10.3390/en8053455.

[47] Gueymard CA. SMARTS2, Simple model of the atmospheric radiative transfer of sunshine: algorithms and performance assessment. vol. FSEC-PF-27. Report FSEC-PF-270-95, Florida Solar Energy Center, Cocoa, FL.: Florida Solar Energy Center; 1995.

[48] Gueymard CA. The SMARTS spectral irradiance model after 25 years: New developments and validation of reference spectra. Solar Energy 2019;187:233–53. doi:10.1016/J.SOLENER.2019.05.048.

[49] Gueymard CA. Prediction and validation of cloudless shortwave solar spectra incident on horizontal, tilted, or tracking surfaces. Solar Energy 2008;82:260–71. doi:10.1016/j.solener.2007.04.007.

[50] Holben BN, Eck TF, Slutsker I, Tanre D, Buis JP, Setzer A, et al. AERONET : A federated instrument network and Data archive for aerosol characterization. Remote Sensing of Environment 1998;66:1–16.

[51] Cabrera Reina A, Miralles-Cuevas S, Cornejo L, Pomares L, Polo J, Oller I, et al. The influence of location on solar photo-Fenton: Process performance, photoreactor scaling-up and treatment cost. Renewable Energy 2020;145:1890–900. doi:10.1016/j.renene.2019.07.113.

[52] Caballero JA, Fernández EF, Theristis M, Almonacid F, Nofuentes G. Spectral Corrections Based on Air Mass, Aerosol Optical Depth, and Precipitable Water for PV Performance Modeling. IEEE Journal of Photovoltaics 2018;8:552–8. doi:10.1109/JPHOTOV.2017.2787019.

[53] Ishii T, Otani K, Itagaki A, Utsunomiya K. A simplified methodology for estimating solar spectral influence on photovoltaic energy yield using average photon energy. Energy Science & Engineering 2013;1:18–26. doi:10.1002/ese3.3.

[54] Litjens G. Investigation of Spectral Effects on Photovoltaic Technologies by Modelling the Solar Spectral Distribution. 2013.

[55] IEC 60904-7. Photovoltaic devices e part 7: computation of the spectral mismatch correction for measurements of photovoltaic devices. International Electrotechnical Commission (IEC), Geneva, Switzerland,; 2008.

[56] Finkelstein JM, Schafer RE. Improved goodness-of-fit tests. Biometrika 1971;58:641–5. doi:10.1093/biomet/58.3.641.

[57] Izenman AJ. Modern Multivariate Statistical Techniques : regression, classification, and manifold learning. Springer-Verlag New York; 2016.

[58] Gueymard CA. A review of validation methodologies and statistical performance indicators for modeled solar radiation data: Towards a better bankability of solar projects. Renewable and Sustainable Energy Reviews 2014;39:1024–34. doi:10.1016/j.rser.2014.07.117.